

# THE INFLUENCE OF IRON OXIDE ON THE STRUCTURAL AND OPTICAL PROPERTIES OF BOROSILICATE GLASSES

Fawzeya Gharghar<sup>1\*</sup> and Sammer El-Jadal<sup>2</sup>

<sup>1</sup> Department of Physics, Faculty of Education – Qaser Bin Ghasher, Tripoli University, Libya

<sup>2</sup> Department of Physics, Faculty of Education – Ajaylat, Zawya University, Libya

\* [fawzeyagharghar@gmail.com](mailto:fawzeyagharghar@gmail.com)

## Abstract

Borosilicate glasses containing  $\text{Fe}_2\text{O}_3$  with the chemical composition  $30\text{Na}_2\text{O} - 2\text{Al}_2\text{O}_3 - 25\text{SiO}_2 - x\text{Fe}_2\text{O}_3 - (43-x) \text{B}_2\text{O}_3$  have been prepared and studied over a wide range of concentrations. The impact of such oxide on optical and physical properties of the present system has been examined. The further replacement of  $\text{Fe}_2\text{O}_3$  instead of  $\text{B}_2\text{O}_3$  generally increases the density and molar volume due to the change in the internal structure of the glass network. The optical variation was interpreted according to the observed incorporation of iron oxide and the possible mechanism of non-bridging oxygen in silicate and bridging bonds in borate network. The investigated samples in this study were confirmed to be amorphous by means of XRD, which proved that there are no natural crystal contents.

**Keywords:** Borosilicate; Transition Metals; Iron Oxide; Optical Absorption.

## Introduction

Borosilicate glasses are technologically interesting materials (Konijnendijk W. et al. 1976, Gautam C. et al. 2013) as they are widely used in industry for various applications. Its scientific and technological importance owing to the combination of stability advantages of silicate glass and the lower melting point with good transparency, besides the high chemical and thermal stability of borate glass. For these reasons, borosilicate glass is approved (El-Damrawi G. et al. 2016, Ebrahimi E. et al. 2018) as the material of choice for many applications as a substitution for quartz products, in laboratory ware and pharmaceutical containers, and to develop highly efficient luminescence and optical materials.

Borosilicate glasses have been widely explored (Gautamet al. 2013, El-Damrawi. et al. 2016, and Ebrahimiet al. 2018) by many researchers. Spectroscopic observations indicated that, borosilicate glasses have mixed network formers and their local environments is based on the main building units of silica  $\text{Q}^n$  [ $\text{SiO}_4$ ] units - where n is the number of bridging oxygen atoms per tetrahedron- and the triangular [ $\text{BO}_3$ ] and the tetrahedral [ $\text{BO}_4$ ] of boron units. The [ $\text{BO}_3$ ] units are triangle boron in both

ring and non-ring configurations, while four-coordinated ( $\text{BO}_4$ ) units are boron atoms in tetrahedral coordination.

Furthermore, borosilicate glasses containing transition metal ions (TMI) such as iron, copper, cadmium, and vanadium have received more attention because they generally have interesting optical, electrical and magnetic properties. These properties are utilized in many useful fields, such as tunable solid-state lasers, phosphors, solar energy converters, plasma display panels, electronic and optical devices.

Many interesting investigations are available regarding the environment of TMI in different glass systems (Elbashar Y. et al. 2017, Abdelghany A. et al.2012, and Bhogi A. et al.2016). It was reported that, iron ions exist in two valence states, divalent  $\text{Fe}^{+2}$  (ferrous ions) when it plays the network modifier role and trivalent  $\text{Fe}^{+3}$  (ferric ions) when it strengthens the network structure more like a network former. The relative amounts of both ions depend on the melting condition, type and concentrations of glass compounds.

El-Damrawi G.et al. (2016) revealed that the presence of low content of iron oxide is consumed to modify borosilicate network due to the formation of NBOs units in silicate network and to the transformation of  $\text{BO}_3$  to  $\text{BO}_4$  species.

FTIR analyses indicated that the fraction  $N_4$  of four coordinated boron atoms was found to increase up to 6 mol% iron oxide, then a significant decrease is observed in  $N_4$  with an increase in  $\text{Fe}_2\text{O}_3$  contents (>6 mol%). This confirms that iron oxide enters the glass network as a glass network former at high concentration and plays the role of the main glass modifier in the low- $\text{Fe}_2\text{O}_3$  region.

The present work mainly focuses on studying the physical and optical properties of the  $\text{Fe}_2\text{O}_3$  incorporated sodiualumino-borosilicate glassy system. The variation of physical properties such as density and molar volume with increasing iron oxide has been evaluated over a wide range of concentrations.

Ultraviolet-visible (UV-Vis) technique was carried out to identify the spectral contribution of iron ions within the structure and to highlight the role of the iron ions as a modifier of the glass network.

### **Experimental Method**

Iron borosilicate glasses of the formula  $x\text{Fe}_2\text{O}_3.(43-x) \text{B}_2\text{O}_3.25\text{SiO}_2.30\text{Na}_2\text{O}.2\text{Al}_2\text{O}_3$  were prepared by melting a batch with appropriate amounts of the raw materials:  $\text{Fe}_2\text{O}_3$ ,  $\text{Al}_2\text{O}_3$ , and  $\text{SiO}_2$ .  $\text{Na}_2\text{O}$  was added as sodium carbonate and  $\text{B}_2\text{O}_3$  as orthoboric acid ( $\text{H}_3\text{BO}_3$ ). The weighed chemical batches mixed and melted in crucibles using an electric furnace at temperature ranged between 1250 and 1550 °C, depending on the glass composition. The melted glasses were stirred for several times until a complete

homogenization was obtained. The homogenized melt was then poured in warmed stainless steel molds of the required dimensions.

X-ray diffraction patterns (XRD) were performed at Central Metallurgical Research and Development Institute (CMRDI), El-Tebbeen- Helwan using a Bruker Axs-D8 Advance powder. The range of the diffraction angle  $2\theta$  is changed from  $4^\circ$  to  $70^\circ$  with a dwell time of 0.4 seconds using computer-controlled X-ray diffractometer with Cu Ka radiation source.

The optical absorption spectra were recorded on polished disk-shaped samples at room temperature using a UV-visible spectrophotometer (Cary-50), working in the wavelength range 190–1100 nm and using a computerized double beam spectrophotometer.

Density of the glass samples was conducted experimentally to investigate the impact of  $\text{Fe}_2\text{O}_3$  replacing  $\text{B}_2\text{O}_3$  on the glass structure.

Standard Archimedes method (Elbashar Y. et al. 2017, Bhogi A. et al., 2016, and Zhu C. et al., 2017) was used to evaluate the density by using xylene as an immersion liquid as follow:

$$D = (W_{SA} - W) * DL / (W_{SA} - W_{SL}) \quad (1)$$

$W_{SA}$  and  $W_{SL}$  are the weights of the sample in the air and xylene respectively.  $W$  is their weight in air and  $D_L$  is the density of xylene liquid.

The density data were used to calculate the molar volume ( $V_m$ ) using the relation:

$$V_m = M/D \quad (2)$$

Where  $M$  is the relative molecular mass of glass

## Results and Discussion

The dependence of density ( $D$ ) and molar volume ( $V_m$ ) on  $\text{Fe}_2\text{O}_3$  concentration is plotted in Figure (1). It has been noticed that the density values are gradually increased with iron ions contents from  $\sim 2.49$  to  $2.9 \text{ g/cm}^3$ . This behavior may be attributed to the addition of heavier Fe atoms instead of lighter B since the density of glass is very sensitive to the ionic size and atomic weight (El-Damrawi G. et al., 2016, Ebrahimi E. et al., 2018, and Zhu C. et al., 2017). Besides, the presence of iron oxide is used to modify the structural network by providing more oxygen, thus it allows more conversion from the  $\text{BO}_3$  triangular to  $\text{BO}_4$  tetrahedral units (Bhogi A. et al., 2016, Bjaoui N. et al., 2021, and Rus L. et al., 2014). In such a case, formation of denser tetrahedral bonds, rather than the local glass linkage, leads to a significant enhancement in the density of the prepared samples.

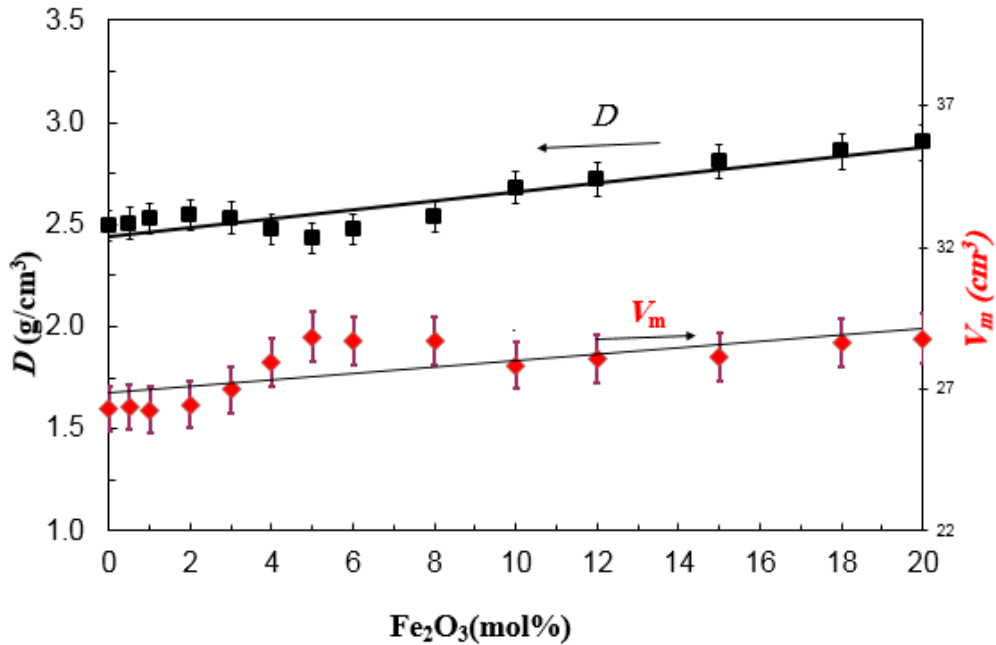


Figure (1): Variation of Density and Molar Volume with Fe<sub>2</sub>O<sub>3</sub> Content.

The increase in glass density is followed by an increase in molar volume as shown in Figure (1). In this case, the replacement of B<sub>2</sub>O<sub>3</sub> by Fe<sub>2</sub>O<sub>3</sub> causes the glass structure less compact due to the larger structural size of BO<sub>4</sub> rather than BO<sub>3</sub> structural units and due to the formation of NBO units in silicate side.

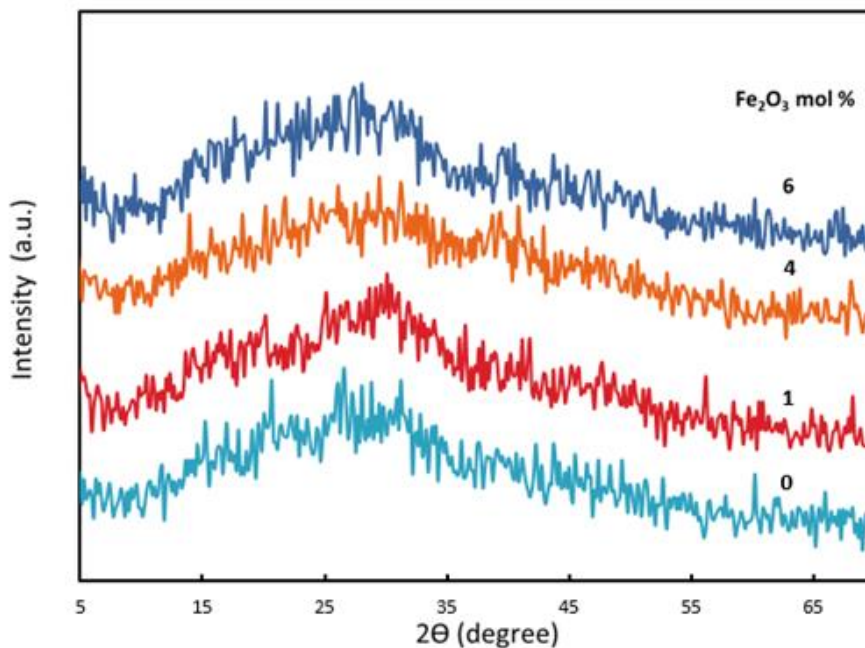


Figure (2): X-ray Diffraction Graph of Iron-Borosilicate Glass System.

The measured X-ray powder diffraction pattern (XRD) of an amorphous material is fundamentally different from that of a crystalline material. The crystalline component is characterized by sharp x-ray distinguished peaks, whereas, the amorphous content exhibits few broad diffuse halos.

XRD pattern for some selected samples is shown in Figure (2). The outcomes demonstrate the long-range disorder arrangement and the absence of sharp peaks in XRD spectra. This confirms that the present samples are completely amorphous and do not present any crystalline phase.

The optical absorption spectra of the selected glasses have been carried out at room temperature over the wavelength range in the UV-visible (190-1100nm) region. Figure (3) illustrates the wavelength dependence of the absorption spectra for some prepared glass samples. That can be observed, by increasing Fe<sub>2</sub>O<sub>3</sub> content, the absorbance of UV light is increased toward higher wavelengths from about ~300 nm at 0 mol% to about ~400 nm at 6 mol%. Moreover, the incorporation of Fe<sub>2</sub>O<sub>3</sub> in the host matrix induces additional absorption band in the UV and visible regions appearing between 400 and 600 nm, which correspond to the absorption of iron ions (Bhogi A. et al., 2016, Bjaoui et al., 2021, and Rus et al., 2014). The intensity of this band is observed to increase as the concentration of Fe<sub>2</sub>O<sub>3</sub> is increased from 0 to 6 mol%.

According to several researches (Elbashar Y. et al., 2017, Abdelghany A. et al., 2012), iron based glasses possess an interesting optical spectrum at both ultraviolet and visible-near infrared regions due to the iron–oxygen charge transfer. It has been observed that the most important UV–Vbands associated with the Fe<sup>+2</sup> ions are having a band in the ultraviolet region, another one in the visible range in the 450–550 nm region and the last one in the infrared region at about 1050nm (Zhu C. et al., 2017, Bjaoui et al., 2021, Rus et al., 2014). Thus, the gradual increase of Fe<sub>2</sub>O<sub>3</sub> content leads to a widening of the band situated in 450–550 nm region towards red color domain indicates that the number of Fe<sup>+2</sup> ions increases as a result of the dominant role that played by Fe<sub>2</sub>O<sub>3</sub>. This observation is in good agreement with the previous NMR and FTIR investigations (El-Damrawi G. et al., 2016).

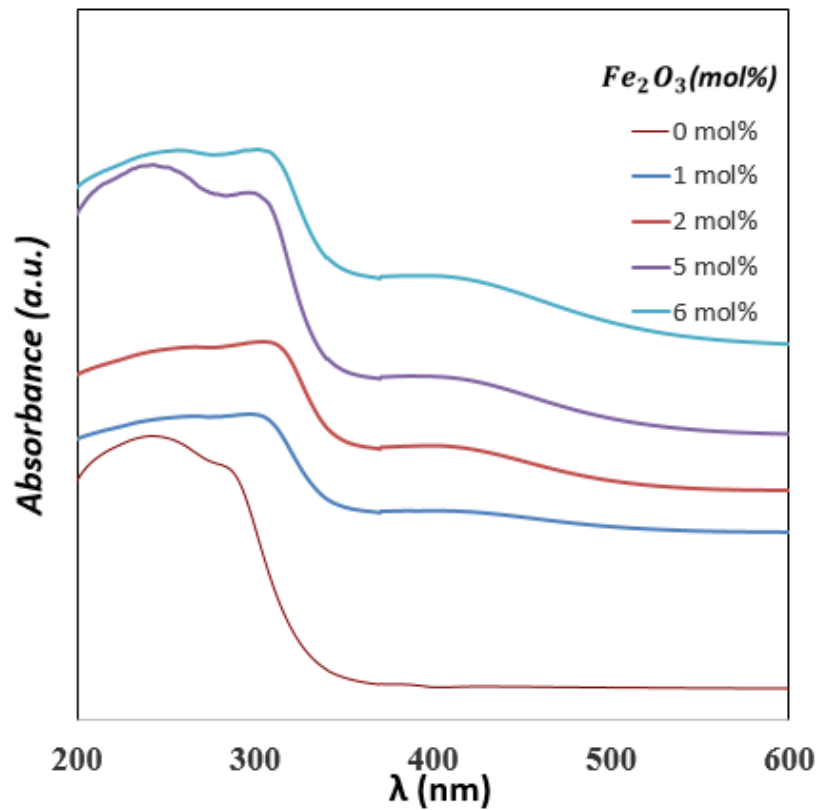


Figure (3): UV-V is Absorption Spectra of Iron-Borosilicate Glass System.

Studying the optical properties is very useful to get information about the band structure and energy gap of noncrystalline materials (Elbashar Y. et al., 2017, Bhogi A. et al., 2016).

Urbach (Zhu C. et al., 2017, Bjaoui N. et al., 2021) found that the absorption coefficient  $\alpha(\nu)$  depends exponentially on the photon energy ( $h\nu$ ) according to:

$$\alpha(\nu) = B \exp \left[ \frac{h\nu}{E_U} \right] \quad (3)$$

where  $h$  is Planck's constant,  $\nu$  the frequency of incident photons and  $E_U$  the Urbach energy.

Measurement of  $\alpha(\nu)$  as a function of the optical absorbance  $A$  and the sample thickness  $d$  was determined from the relation:

$$\alpha(\nu) = 2.303 \frac{A}{d} \quad (4)$$

The optical band gap  $E_g$  can be determined using Tauc expression as follows:

$$\alpha(\nu) = B \frac{(h\nu - E_g)^n}{h\nu} \quad (5)$$

Where B is constant depending on transition probability, the value of n determines the nature of optical transition where  $n = \frac{1}{2}$  indicates direct transition and  $n = 2$  indicates indirect transition. The relation between  $(\alpha h\nu)^{1/2}$  and the photon energy ( $h\nu$ ) was obtained and given in Figure (4).

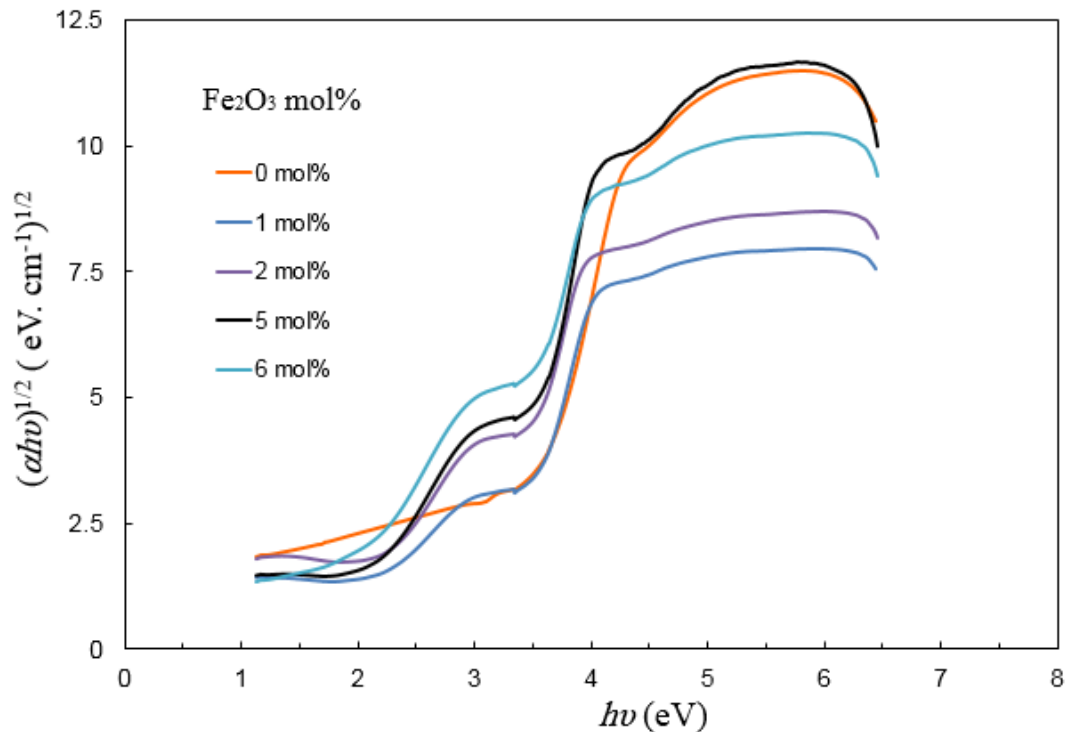


**Figure (4): Variation of  $(\alpha h\nu)^{1/2}$  as a Function of Photon Energy ( $h\nu$ ) for the Studied Glasses.**

Plots also were drawn between  $\ln \alpha$  and  $h\nu$  as shown in Figure (5). As a result, the Urbach energy of the present system can be obtained (eq3) as  $1/\text{slope}$  of the straight-line part of the curves in  $\ln(\alpha)$  vs  $h\nu$  plot. Figure (6) presents the variation of the Urbach energy as function of iron oxide concentration. The results showed a slight increase in  $E_U$  from 0.303eV to 0.357eV when substituting boron oxide for iron oxide. In this regard, the increase in  $E_U$  may be related to the structural variation and to the increase in the degree of disorders in glass structure. The replacement of  $B_2O_3$  by  $Fe_2O_3$  ( $x \leq 6$  mol%) in the present system is expected to make the network structure more open and enhance the modification process in the glass environment.

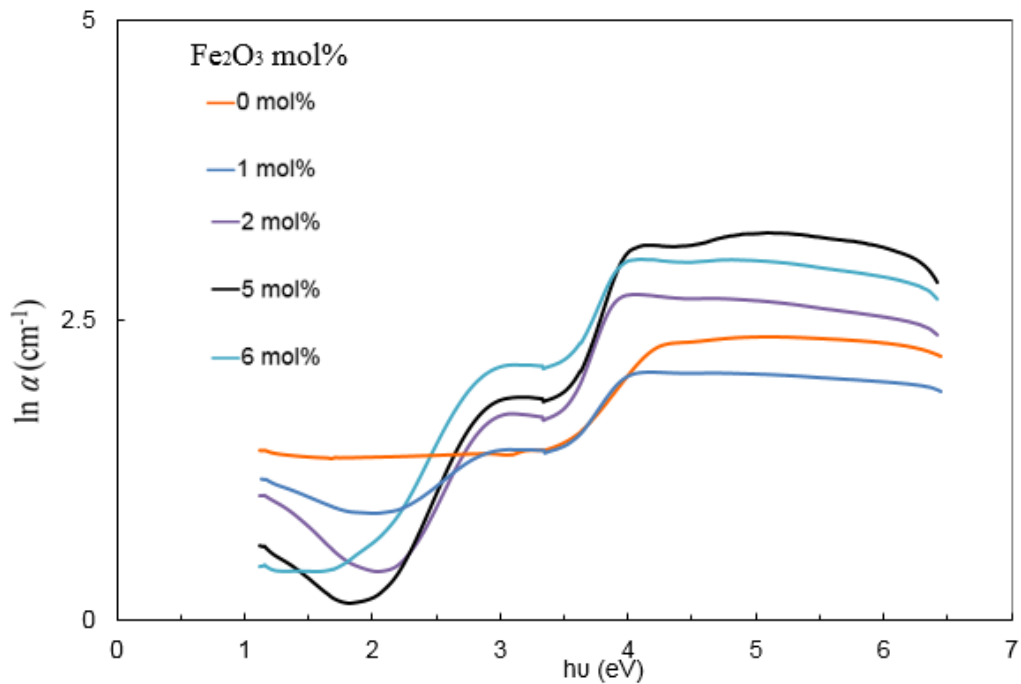


**Figure (5): Variation of  $\ln \alpha$  as a Function of Photon Energy ( $h\nu$ ) for the Studied Glasses.**

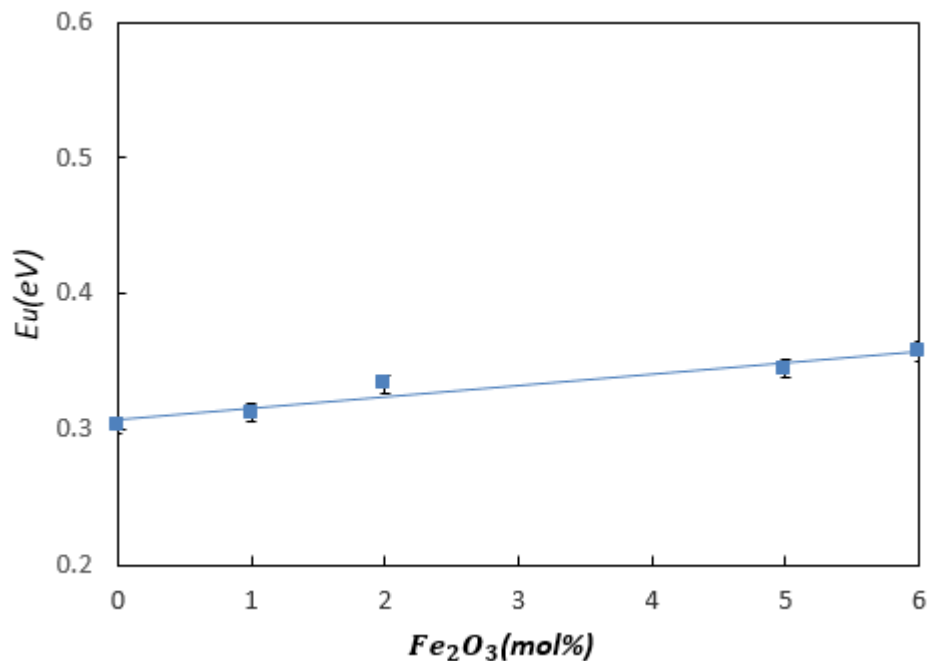


**Figure (6): Variation of Urbach Energy ( $E_U$ ) vs  $Fe_2O_3$  mol%.**

Using the above equations, the energy gap can be calculated by extrapolating the straight-line portion to cut the energy axis to zero absorption in the  $(\alpha h\nu)^{1/2}$  versus  $h\nu$  plot. Figure (7) shows an example for obtaining the value of optical band gap  $E_g$  ( $Fe_2O_3=2\text{mol}\%$ ).



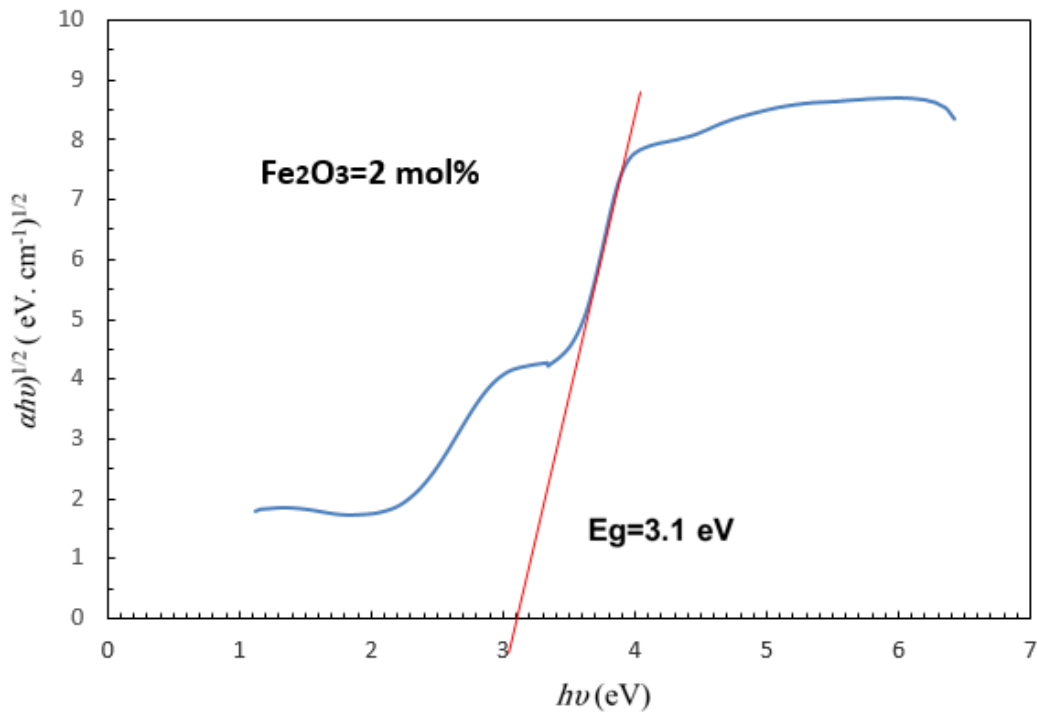


**Figure (7): An Example for Determination of the Optical Band Gap.**

The refractive index is utilized to evaluate the suitability of glassy materials to be optical devices. The refractive index ( $n$ ) of the investigated glasses can be deduced from the band gap ( $E_g$ ) using the following relation:

$$\frac{n^2-1}{n^2+2} = 1 - \sqrt{\frac{E_g}{20}} \quad (6)$$

The effect of iron concentration on both ( $E_g$ ) and ( $n$ ) is presented in Figure (8) and tabulated in Table (1). It is known that the variation of energy gap with glass composition is significantly correlated with the creation of non-bridging oxygen ions in the base glass network (Ebrahimi E. et al., 2018, Elbasha Y. et al., 2017, and Rus L. et al., 2014). The decreasing in ( $E_g$ ) from 3.35 to 3eV may be attributed to breaking the local boron bonds and formation of NBOs in silicate network as a result of the modification process.

**Table (1): The Physical and Optical Parameter Values of Iron Borosilicate Glasses: Molar Volume  $V_m$ , Urbach Energy  $E_u$ , Optical Band Gap  $E_g$ , Linear Refractive Index  $n$ , Molar Refractivity  $R_m$ , Metallization Criterion  $M$ .**

$Fe_2O_3$ (mol%)	$V_m$	$E_u$	$E_g$	$n$	$R_m$	$M$
0	26.32	0.303	3.35	2.309	15.55	0.41
1	26.272	0.316	3.29	2.323	15.62	0.41
2	26.461	0.333	3.1	2.371	16.04	0.4
5	28.845	0.345	3.15	2.358	17.40	0.4
6	28.709	0.357	3	2.397	17.59	0.39

Furthermore, the refractive index  $n$  is found to increase with the addition of  $Fe_2O_3$ . This can be related to the difference in ion refraction of B and Fe. It is known that, the ion refraction of Fe is higher than that of B; this explains the increase of refractive index by increasing  $Fe_2O_3$  content. Besides, the formation of more NBOs is expected to increase the refractive index of the investigated system (Azlan M. et al., 2014, Dimitrov V. et al., 1996).

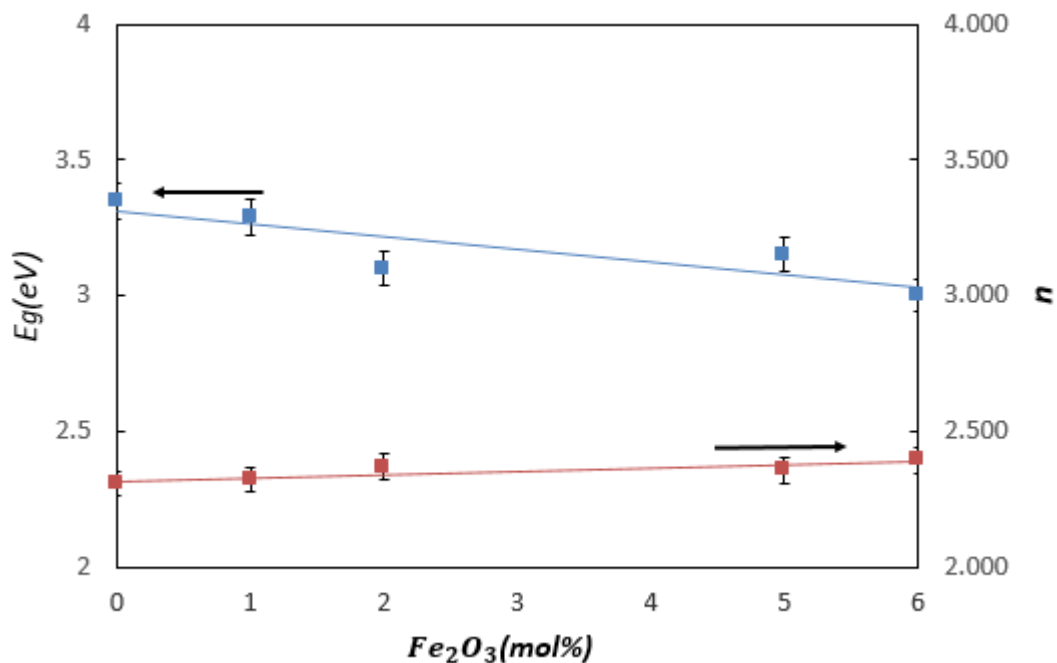


**Figure (8): The Dependence of the Optical Ban Gap  $E_g$  and the Refractive Index  $n$  on  $Fe_2O_3$  mol%.**

In addition, the molar refractive index could be expressed in terms of molar volume ( $V_m$ ), and refractive index ( $n$ ) using the following expression:

$$R_m = \left( \frac{n^2-1}{n^2+2} \right) V_m \quad (7)$$

Metallization criterion of a material can be deduced from the molar refractivity ( $R_m$ ) and the molar volume ( $V_m$ ) using the relation below:

$$M = 1 - \frac{R_m}{V_m} \quad (8)$$

The variation of molar refractivity ( $R_m$ ) and metallization criterion ( $M$ ) by changing the molar fraction of  $Fe_2O_3$  is shown in Figure (9). We obviously observe an inverse proportional relationship between  $R_m$  &  $M$  on basis of  $Fe_2O_3$  content. The molar refraction values increased by the addition of  $Fe_2O_3$  into the borosilicate network because if the increase in the molar volume as shown in Eq (7).

It is noteworthy to point out that, the metallization criterion may also computed based on the band gap energy according to the following formula  $M$  (Abdo M. et al., 2021, Samanta B. et al., 2017):

$$M(E_g) = \sqrt{E_g/20} \quad (9)$$

Therefore, the reduction of ( $E_g$ ) by increasing  $Fe_2O_3$  content resulted in decreasing ( $M$ ) as well.

Based on the obtained metallization criterion value ( $M \sim 0.4$ ), it can be suggested that the glass samples under consideration serve as semiconducting materials (Farhan S. 2017).

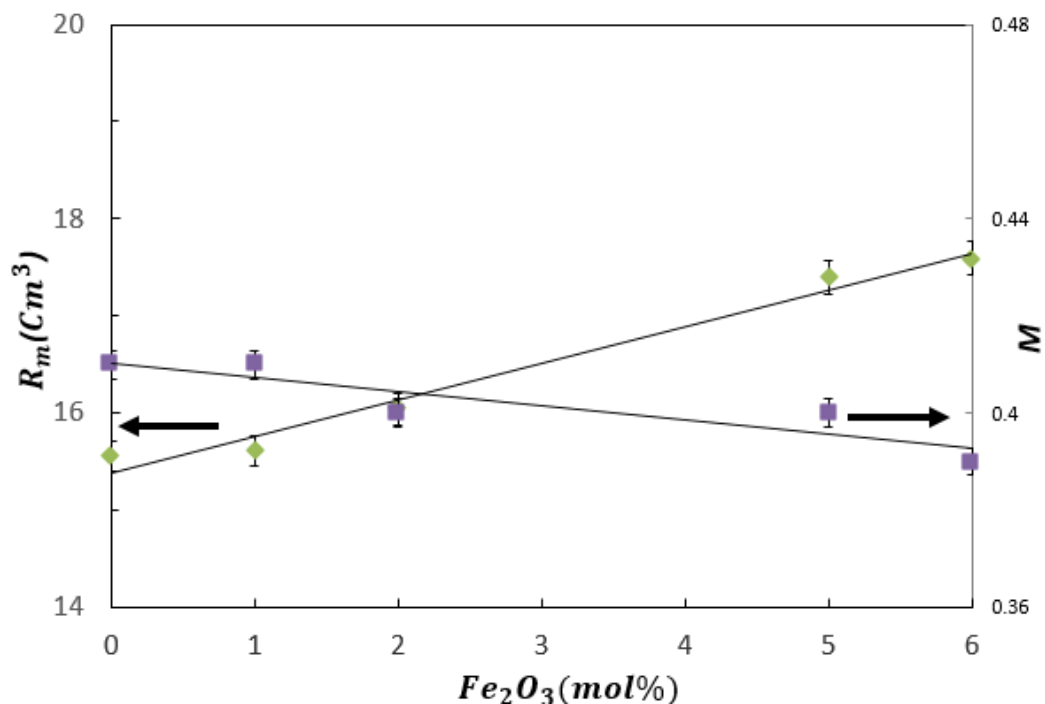


**Figure (9): Variation of molar refractive index and metallization criterion with mol% of  $Fe_2O_3$ .**

## Conclusion

Addition of  $Fe_2O_3$  at the expense  $B_2O_3$  was shown to cause a significant impact on the optical and structural properties of borosilicate glasses. The following conclusions can be drawn:

The widening of the fundamental absorption bands towards higher wave numbers indicates that the number of  $Fe^{2+}$  ions increases at the expense of  $Fe^{3+}$  ions. This result corresponds mainly to the structural modification process that takes place upon introducing  $Fe_2O_3$  at expense of  $B_2O_3$  inside the glass network. XRD patterns of some selected samples did not present any crystalline phases, which confirm the amorphous nature of the investigated glasses. The present study showed that both density and the corresponding molar volume of the prepared glasses increased with the continuous increase of iron oxide. Addition of  $Fe_2O_3$  content up to 6mol% led to increase in the concentration of lattice modification ions, hence transforming borate triangular units, into denser, to larger and stronger tetrahedras. Besides, the difference in the relative atomic masses of Fe and B is an expected reason for the enhancement of the investigated glass density. The incorporation of iron ions into the borosilicate structure reduces energy band gap and results in better light absorption in Uv-Vis regions. The Urbach energy values increase indicates the increase of disorder degree of host matrix. Moreover, molar refractive index  $R_m$  and metallization criterion  $M$  have a reverse trend with the increase of  $Fe_2O_3$  content.

The increment in ( $R_m$ ) is due to the increase in ( $V_m$ ) whereas the small reduction in ( $M$ ) correlated with ( $E_g$ ) decrease. The obtained value of ( $M$ ) reveals that the investigated samples have semiconductor behavior.

## References

- Konijnendijk W, Stevels J. (1976). The structure of borosilicate glasses studied by Raman scattering. *Journal of Non-Crystalline Solids*. 20: 193-224.
- Gautam C, Yadav A. (2013). Synthesis and optical investigations on (Ba, Sr)  $TiO_3$  borosilicate glasses doped with  $La_2O_3$ .
- El-Damrawi G, Hassan A, Ramadan R; El-Jadal S. (2016). Nuclear magnetic resonance and FTIR structural studies on borosilicate glasses containing iron oxide. *new Journal of Glass and Ceramics*. 6: 47.
- Ebrahimi E, Rezvani M (2018). Optical and structural investigation on sodium borosilicate glasses doped with  $Cr_2O_3$ . *Spectrochimica Acta Part A: Molecular and Biomolecular Spectroscopy*. 190: 534-538.
- Elbashar Y, El-Ghany A. (2017). Optical spectroscopic analysis of  $Fe_2O_3$  doped CuO containing phosphate glass. *Optical and Quantum Electronics*. 49: 1-13.
- Abdelghany A, El Batal F, Azooz M.et al. (2012). Optical and infrared absorption spectra of 3d transition metal ions-doped sodium borophosphate glasses and effect of gamma irradiation. *Spectrochimica Acta Part A: Molecular and Biomolecular Spectroscopy*. 98: 148-155.
- Bhogi A, Kumar R, and Kistaiah P.(2016). Physical and optical absorption studies of  $Fe^{3+}$ -ions doped lithium borate glasses containing certain alkaline earths. In *AIP Conference Proceedings*. 1731: 070038.
- Zhu C, Liu J, Huang S, et al. (2017). The Effects of  $Fe_2O_3$  and  $B_2O_3$  on the Glass Structural, Thermal, in Vitro Degradation Properties of Phosphate Based Glasses. *New Journal of Glass and Ceramics*. 7: 100.
- Bjaoui N, Sdiri N, Valente M, et al. (2021). Effects of  $Fe_2O_3$  substitution for  $K_2O$  on the physical properties of  $88P_2O_5-xFe_2O_3-2CoO-(10-x) K_2O$  glasses, *Boletín de la Sociedad Española de Cerámica y Vidrio*. 60: 13-28.

- Rus L, Rada S, Rednic V. et al. (2014). Structural and optical properties of the lead based glasses containing iron (III) oxide. *Journal of non-crystalline solids*. 402: 111-115.
- Azlan M, Halimah M, Shafinas S, Daud W (2014). Polarizability and optical basicity of Er<sup>3+</sup> ions doped tellurite based glasses, *Chalcogenide Lett.* 11: 319.
- Dimitrov V, Sakka S (1996). Electronic oxide polarizability and optical basicity of simple oxides .I. *Journal of Applied Physics*. 79:1736-1740.
- Abdo M, Basfer N, Sadeq M (2021). The structure, correlated vibrations, optical parameters and metallization criterion of Mn–Zn–Cr nanoferrites. *Journal of Materials Science: Materials in Electronics*. 32: 15814-15825.
- Samanta B, Dutta D, Ghosh S. (2017). Synthesis and different optical properties of Gd<sub>2</sub>O<sub>3</sub> doped sodium zinc tellurite glasses. *Physica B:Condensed Matter*. 515: 82-88.
- Farhan S (2017).Study of some physical and optical properties of Bi<sub>2</sub>O<sub>3</sub> TeO<sub>2</sub> V<sub>2</sub>O<sub>5</sub> glasses. *Australian J. of Applied Science*. 11: 171-178.